NH Tautomerism in the Natural Chlorin Derivatives

Juho Helaja,[†,‡] Maria Stapelbroek-Möllmann,[†] Ilkka Kilpeläinen,[‡] and Paavo H. Hynninen*[,†]

Department of Chemistry, University of Helsinki, P.O. Box 55, FIN-00014 University Helsinki, Finland, and Institute of Biotechnology, University of Helsinki, P.O. Box 56, FIN-00014 University Helsinki, Finland

Received December 9, 1999

The NH tautomerism of five Mg-free chlorophyll *a* and *b* derivatives **2**−**6** was studied utilizing NMR spectroscopy and molecular modeling. The results from the dynamic NMR measurements of the chlorins revealed that substituent effects contribute crucially to the free energy of activation ($\Delta G^{\ddagger}$) in the NH tautomeric processes. An intermediate tautomer for the total tautomeric NH exchange in a chlorin was observed for the first time, when the ^{1}H NMR spectra of chlorin e_6 TME (**3**) and rhodin g_7 TME (**4**) (TME = trimethyl ester) were measured at lower temperatures. The lower energy barriers ($\Delta G_1^{\ddagger}$) obtained for the formation of the intermediate tautomers of **3** and **4**, assigned to the N_{22}−H, N_{24}−H *trans*-tautomer, were 10.8 and 10.6 kcal/mol, respectively. The energy barrier ($\Delta G_2^{\ddagger}$ value) for the total tautomeric NH exchange in the five chlorins was found to vary from 13.6 kcal/mol to values higher than 18 kcal/mol. The lowest $\Delta G_2^{\ddagger}$ value (13.6 kcal/mol) was obtained for rhodochlorin XV dimethyl ester (**2**), which was the only chlorophyll derivative lacking the C_{15} substituent. In the case of chlorins **4** and **5**, the steric crowding around the methoxycarbonylmethyl group at C_{15} raised the $\Delta G_2^{\ddagger}$ activation free-energy to 17.1 kcal/mol. However, the highest energy barrier with $\Delta G_2^{\ddagger} > 18$ kcal/mol was observed for the NH exchange of pyropheophorbide *a* methyl ester (**6**), possessing the macrocycle rigidifying isocyclic ring *E*. Our results demonstrate that the steric strain, arising either from the steric crowding around the bulky substituent at C_{15} or the macrocycle rigidifying isocyclic ring *E*, slows down the NH tautomeric process. We suggest that deformations in the chlorin skeleton are closely connected to the NH tautomeric exchange and that the exchange occurs by a stepwise proton-transfer mechanism via a hydrogen bridge.

Introduction

The NH tautomerism of fully conjugated porphyrins has been widely investigated, including studies of substituent effects.[1−3] It has been suggested that the steric and electronic properties of the peripheral substituents and the basicities of the inner nitrogens are important factors determining the structures of transition states and the activation parameters of an NH tautomeric process.[3] For substituted deuterioporphyrins, it has been shown that the conjugation between the β-pyrrolic substituent (acetyl, vinyl) and the β-pyrrolic double bond outside the aromatic delocalization pathway contributes to the overall stability of the major tautomer.[3]

The NH tautomerism of natural chlorins other than bonellin DME (DME = dimethyl ester) (**1**)[4] is a largely uncovered subject, despite the great importance of chlorins in Nature. The only NH tautomerism investigation of other natural chlorins is the 60 MHz ^{1}H NMR study of chlorin e_6 TME (**3**) by Storm and Teklu.[5] An NH tautomerism study has been reported also for the synthetic 5,10,15,20-tetrakis(*m*-hydroxyphenyl)chlorin.[6] In addition, ab initio quantum mechanical calculations have been performed for the chlorin core.[7] No reports concern-

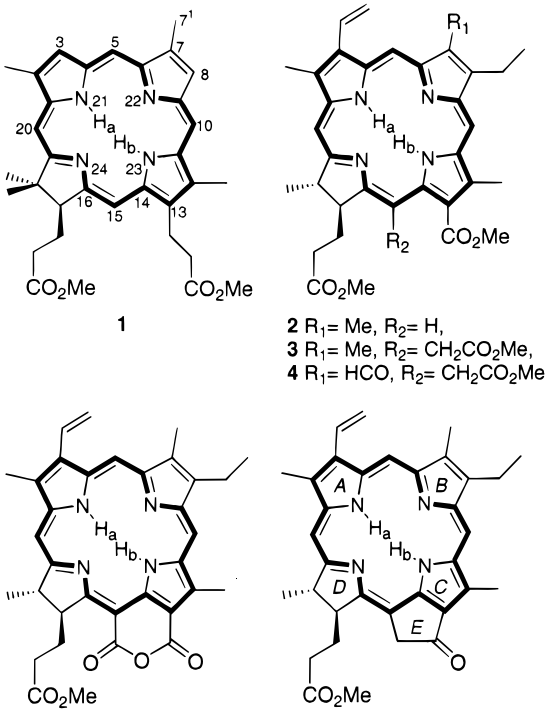

* Corresponding author. FAX: +358-9-19140466. Phone: +358-9-19140358. E-mail: paavo.hynninen@helsinki.fi.
† Department of Chemistry.
‡ Institute of Biotechnology.

(1) Braun, J.; Schlabach, M.; Wehrle, B.; Köcher, M.; Vogel, E.; Limbach, H.-H. *J. Am. Chem. Soc.* **1994**, *116*, 6593 and references therein.
(2) Crossley, M. J.; Field, L. D.; Harding, M. M.; Sternhell, S. *J. Am. Chem. Soc.* **1987**, *109*, 2335.
(3) Crossley, M. J.; Harding, M. M.; Sternhell, S. *J. Org. Chem.* **1992**, *57*, 1833.
(4) Helaja, J.; Montforts, F.-P.; Kilpeläinen, I.; Hynninen, P. H. *J. Org. Chem.* **1999**, *64*, 432.
(5) Storm, C. B.; Teklu, Y. *J. Am. Chem. Soc.* **1972**, *94*, 1745.
(6) Bonnett, R.; Djelal, B. D.; Hawkes, G. E.; Haycock, P.; Pont, F. *J. Chem. Soc., Perkin Trans. 2* **1994**, 1839.

10.1021/jo9918955 CCC: $19.00
Published on Web 05/12/2000

Scheme 1

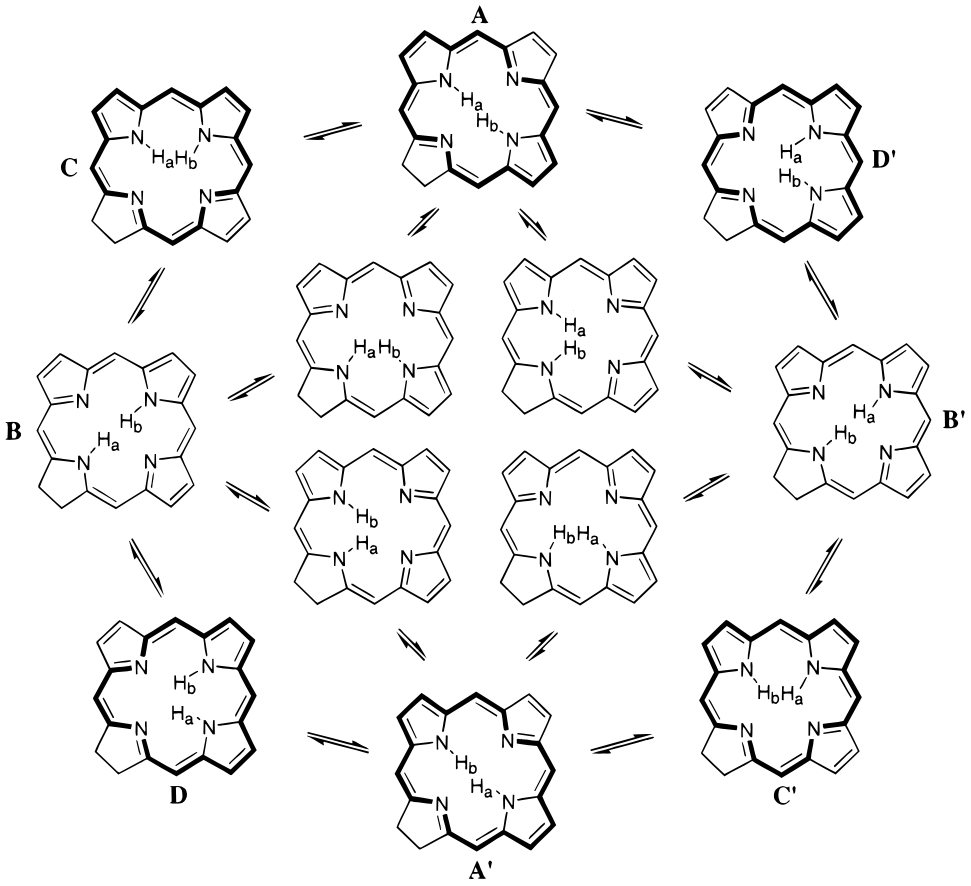

ing the substituent effects on the NH tautomerism in chlorins exist to our knowledge.

We have previously studied the NH tautomerism of **1** by dynamic ^{1}H NMR and molecular modeling.[4] We concluded that the total tautomeric NH exchange, **A** ⇄ **A′**, occurred by a stepwise mechanism via the aromatic *cis*-tautomers **C** and **D** (**C′** and **D′**) and the less aromatic *trans*-tautomer **B** (**B′**) (Scheme 1), with the rate-limiting energy barrier between these *cis*-tautomers and the higher-energy *trans*-tautomer. Using the results from the dynamic ^{1}H NMR measurements and applying the Eyring equation, a value of 14.4 kcal/mol was obtained for the free-energy of activation, $\Delta G_{297}^{\ddagger}$. The semiempirical molecular modeling methods AM1 and PM3 with unrestricted Hartree−Fock (UHF) spin pairing gave structures and energies for the tautomers of chlorin **1**, which were illustrative of the tautomerization mechanism and consistent with the NMR results and also with the molecular modeling results recently calculated by an ab initio method.[8] The AM1-UHF and PM3-UHF methods both favored strongly the chlorin tautomers, in which an aromatic [18]-diazaannulene delocalization pathway is possible without delocalizing the lone-pair electrons of N_{24} in the reduced subring.

In this paper, we present the results from our study of the NH tautomerism in five natural chlorins, comprising the Mg-free derivatives **2**−**6** of chlorophylls (Chl) *a* and *b*. In the study, we have applied the methods that were shown to be informative in the analysis of the NH tautomerism in chlorin **1**. The experimental results were produced by dynamic ^{1}H NMR (DNMR) and ^{1}H−^{15}N NMR heteronuclear measurements. The molecular modeling calculations for the chlorin tautomers were performed using the PM3-UHF method.[4] The aim of this study is to illuminate how different chlorin-ring substituents influence the NH tautomerism.

The substituted chlorins **2**−**6** used in this investigation are related to Chls *a* and *b* as follows. Rhodochlorin XV (3^1,3^2-didehydrorhodochlorin)[9] DME (**2**) is a Mg-free Chl *a* derivative lacking the C_{15} substituent. Chlorin e_6 (3^1,3^2-didehydrorhodochlorin-15-acetic acid)[9] TME (**3**) and rhodin g_7 (3^1,3^2-didehydro-7^1-oxorhodochlorin-15-acetic acid)[9] TME (**4**) are Mg-free derivatives of Chl *a* and *b* in which the isocyclic ring *E* has been opened. Purpurin 18 (3^1,3^2-didehydro-15-carboxyrhodochlorin anhydride)[9] methyl ester (**5**) has a six-membered anhydride ring instead of the isocyclic ring. Pyropheophorbide *a* (3^1,3^2-didehydrophytochlorin)[9] methyl ester (**6**) is a Mg-free derivative of Chl *a*, having an isocyclic ring *E* that appreciably rigidifies the chlorin macrocycle compared with the other derivatives.

Results

^{1}H DNMR Measurements. The dynamic ^{1}H NMR measurements were performed for chlorins **2**−**6** to obtain the energy barriers for the NH tautomeric exchange. The activation free energies, $\Delta G_1^{\ddagger}$ and $\Delta G_2^{\ddagger}$, were calculated in terms of the coalescence temperature (T_{C1} and T_{C2}) and

(7) Almlöf, J.; Fisher, T. H.; Gassman, P. G.; Ghosh, A.; Häser, M. *J. Phys. Chem.* **1993**, *97*, 10964.
(8) Sundholm, D.; Konschin, H.; Häser, M. *Chem. Eur. J.* **1999**, *5*, 267.
(9) International Union of Pure and Applied Chemistry (IUPAC) and International Union of Biochemistry (IUB). *Nomenclature of Tetrapyrroles*; Moss, G. B., Ed.; *Pure Applied Chemistry*; Blackwell: Oxford, U.K., 1987; Vol. 59, p 779.

Table 1. Measured Coalescence Temperatures (T_C), Exchange Rate Constants (k_C), and Activation Free Energies ($\Delta G^{\ddagger}$) for Chl Derivatives in $CDCl_3$

derivative	T_{C1} (K)	k_{TC1}[a] (Hz)	$\Delta G_1^{\ddagger}$[b] (kcal/mol)	T_{C2} (K)	k_{TC2}[a] (Hz)	$\Delta G_2^{\ddagger}$[b] (kcal/mol)
1[4]	nr	nr	nr	297	74	14.4
2	nr	nr	nr	281	162	13.6
3	218	76	10.8	345[c]	109	17.1
4	222	180	10.6	338[d]	105	16.8
5	nr	nr	nr	341[e]	127	16.8
6	nr	nr	nr	>403[f,g]	1465[f]	>18.0

[a] $k_{TC} = \pi\Delta\delta/\sqrt{2}$ Hz. [b] $\Delta G^{\ddagger} = 4.58T_C(10.32 + \log(T_C/k_C))$ cal/mol; nr = not resolved. [c] Measured in pyridine-d_5. [d] Measured in CD_3CN. [e] Measured in dioxane-d_8. [f] Measured in 300 MHz magnetic field in DMSO-d_6. [g] The highest T at which the NH proton signals could be resolved from the baseline.

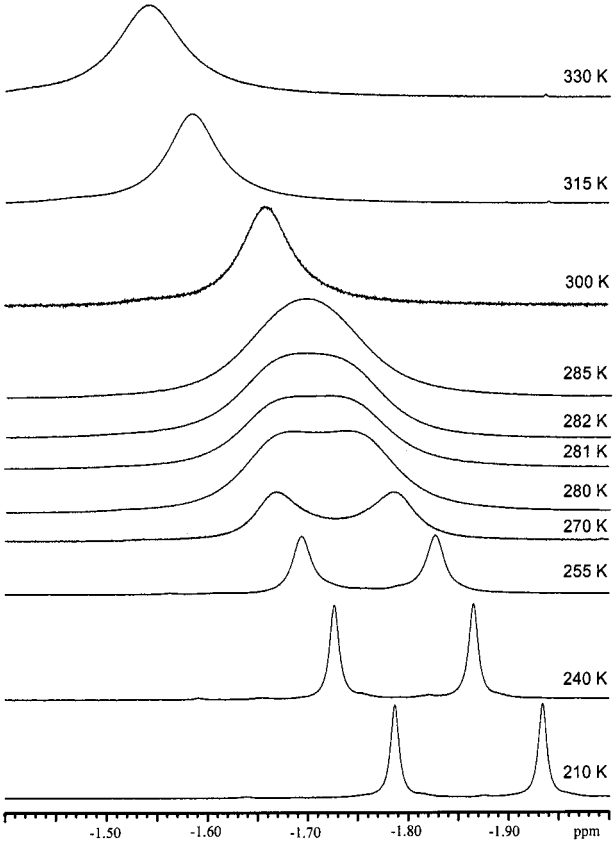

Figure 1. NH part of the variable-temperature ^{1}H NMR spectra of **2** in $CDCl_3$.

the exchange rate constant (k_{TC1} and k_{TC2}) utilizing the Eyring equation[10] (Table 1). Chloroform-d_1 was chosen as a general solvent for the DNMR measurements, because all the chlorins easily dissolved in it. However, at temperatures above 335 K higher-boiling solvents such as 1,4-dioxane-d_8, pyridine-d_5, and dimethyl sulfoxide-d_6 were used.

In the DNMR measurements, a higher coalescence temperature T_{C2} was observed for chlorins **1**−**5** when the N_{21}−H and N_{23}−H signals merged into one signal (Table 1, Figures 1 and 2). For chlorins **3** and **4,** in addition to T_{C2} also a lower coalescence temperature T_{C1} (218 and 222 K, respectively) was observed, indicating that the NH proton signals of some intermediate NH tautomer merged with those of the N_{21}−H, N_{23}−H tautomer (**A** and **A′** in

(10) Friebolin, H. *Basic One- and Two-Dimensional NMR Spectroscopy*; VCH: Weinheim, 1993; p 295.

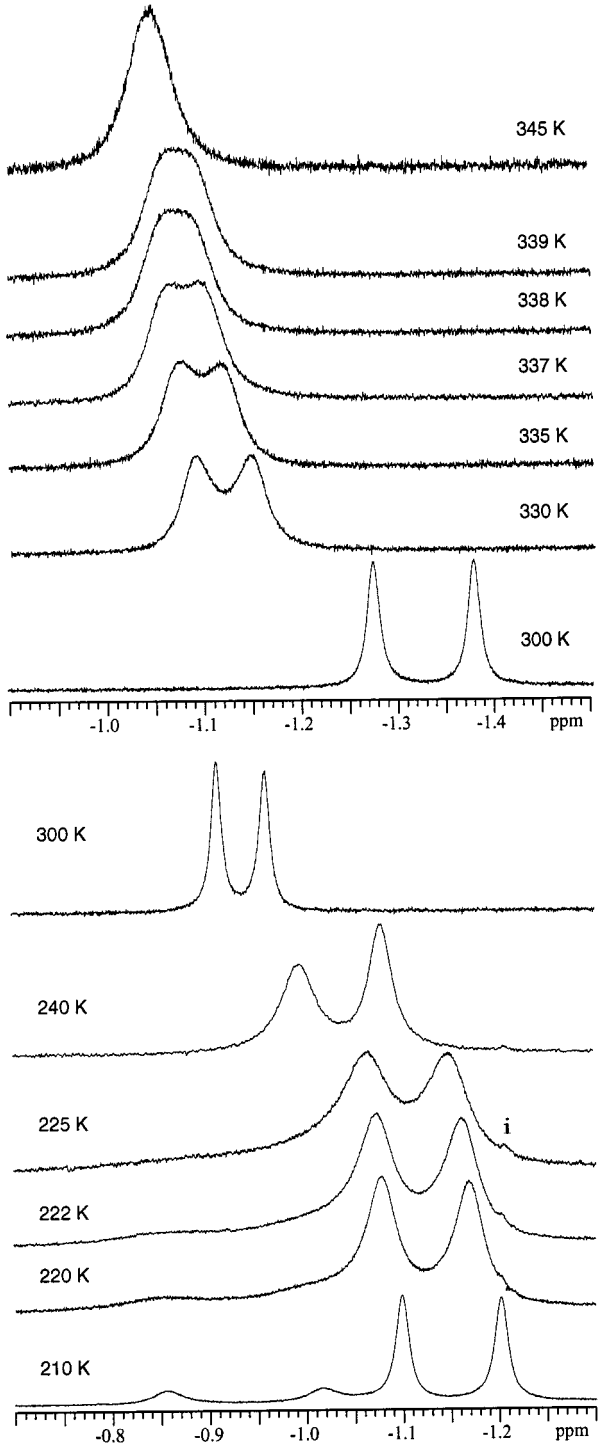

Figure 2. NH part of the variable-temperature ^{1}H NMR spectra of **4** in $CDCl_3$ ($T \leq 300$ K) and in CD_3CN ($T \geq 300$ K), i denotes impurity.

Scheme 1). The higher coalescence temperature T_{C2} can be straightforwardly assigned to the highest energy barrier ($\Delta G_2^{\ddagger} = 17.1$ kcal/mol for **3** and 16.8 kcal/mol for **4**) of the total NH tautomeric exchange, **A** ⇄ **A′**, whereas the lower coalescence temperature T_{C1} apparently corresponds to the lower energy barrier ($\Delta G_1^{\ddagger}$) between a fully aromatic *cis*-tautomer (**C**, **C′**, **D**, **D′**) and the most stable *trans*-tautomer (**A**, **A′**). The lower energy barriers ($\Delta G_1^{\ddagger}$) obtained for chlorins **3** and **4** were 10.8 and 10.6 kcal/mol, respectively (Table 1). The ^{1}H spectra of **4** in Figures 2 and 3 show that the so-far undetected chlorin isomer, the intermediate tautomer (**B**, **B′**), is present with

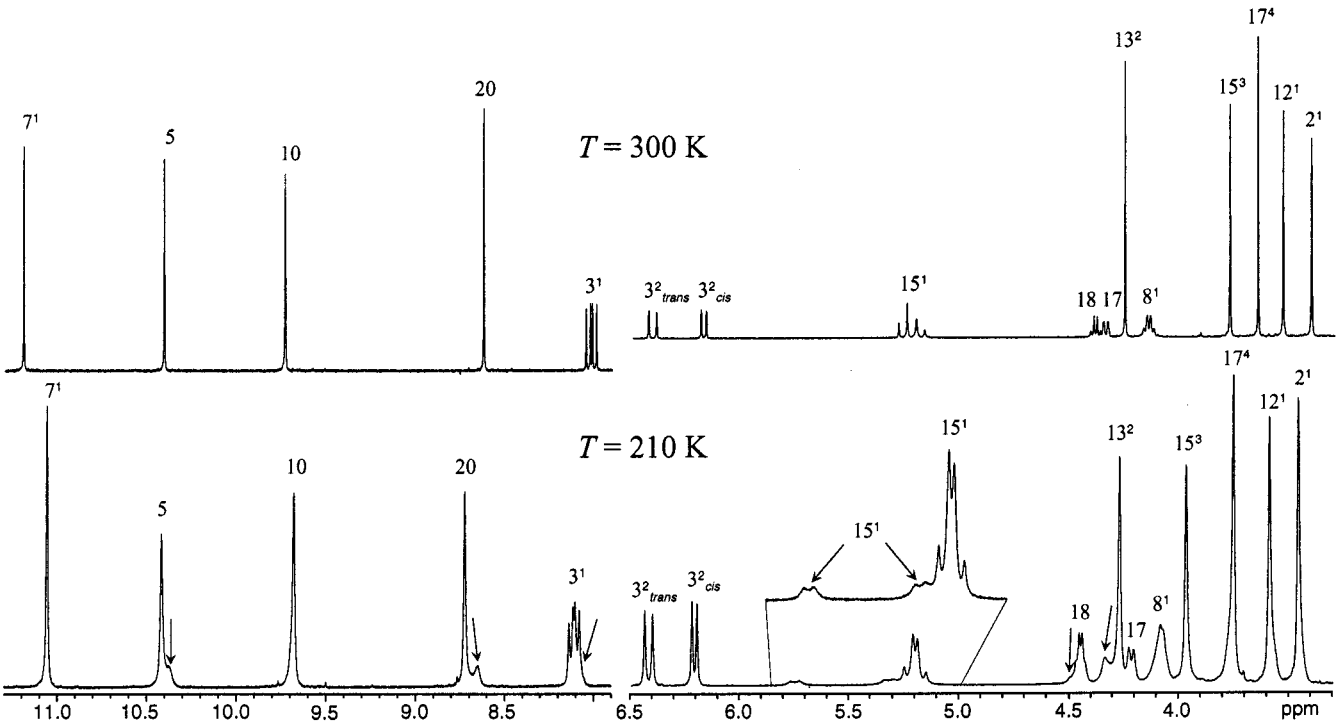

Figure 3. ^{1}H NMR spectra of **4** at 300 and 210 K.

a 15% population, as estimated from the integration values of the NH proton signals.

The NH protons of the observed intermediate tautomer of **3** or **4** were less shielded than those of the major tautomer (Figure 2). This effect can be attributed to a weakening of the ring current. The new isomer exhibited also different δ_H values for several other protons, shown with arrows in Figure 3. We interpret that the differences in the δ_H values were induced either by conformational changes and/or by changes in the π-electron delocalization pathway of the chlorin structure. Apparently, the clear high-field shifts of the 5 and 20 *meso*-proton signals could originate from the latter and the low-field shifts of the 15^1, 18, and 13^2 proton signals from the former changes. The most pronounced changes were observed for the signal arising from the 15^1 methylene protons (Figure 3), which indicates that these protons became clearly chemically nonequivalent in the intermediate tautomer. This effect could originate from the restricted rotation of the C_{15} substituent in the intermediate tautomer at lower temperatures.

The chemical shifts of the NH protons of chlorin **6** in $CDCl_3$ were insensitive to temperature variations (Figure 4), but in DMSO-d_6 the resonances became broader at higher temperatures, and finally disappeared at 403 K. These effects cannot arise from a real coalescence situation, because the NH proton signals did not approach one another upon heating, indicating that the real T_C had not yet been reached. Consequently, we attribute the observed line-broadening to the exchange of the NH protons with the residual water protons in DMSO-d_6. The latter exchange was proven by the addition of 10 μL of D_2O to the chlorin **6** sample in DMSO-d_6, which led to a quantitative exchange of the NH into ND in a few minutes at 300 K.

Figure 4 shows that, in the temperature range of 210−330 K, the NH protons of **2**−**5** become 0.2−0.3 ppm more deshielded in going from the lowest to the highest

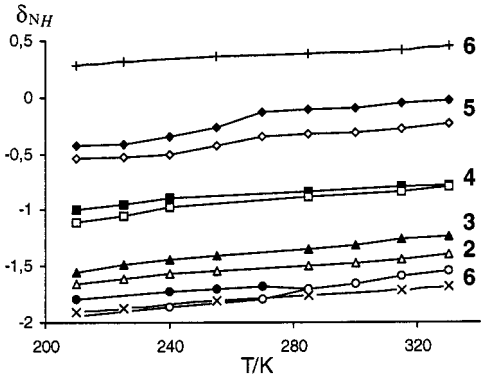

Figure 4. Temperature dependence of δ_{NH} values for chlorins **2**−**6** in $CDCl_3$. The hollow symbols belong to the N_{21}−H and the filled ones to the N_{23}−H protons. The N_{21}−H and N_{23}−H for chlorin **6** are denoted with + and × signs, respectively.

temperature. The δ_{NH}/T dependence was also similar for chlorin **6**. All the chlorins were well soluble in $CDCl_3$ at the concentrations required for ^{1}H NMR. When 20 μL of pyridine-d_5 was added to the chlorin **6** sample in $CDCl_3$, slight low-field shifts were observed for the NH proton signals, but the signals still showed a strong dependence on temperature. For the derivatives soluble in pyridine-d_5, the δ_{NH} values were low-field shifted compared with those measured in $CDCl_3$ but displayed only negligible T dependence. However, the NH protons of chlorin **4** in CD_3CN and those of chlorin **5** in 1,4-dioxane-d_8 showed a temperature-dependent deshielding behavior similar to that observed for chlorins **2**−**6** in $CDCl_3$. Despite the solvent dependence of the δ_{NH} values, we obtained, e.g., for chlorin **5** the same $\Delta G_2^{\ddagger}$ value in pyridine-d_5 as in $CDCl_3$.

^{15}N NMR. The ^{15}N chemical shifts provide information about the electronic surroundings of the central nitrogen atoms, determined by factors such as the chemical types of the nitrogen atoms, the aromatic delocalization path-

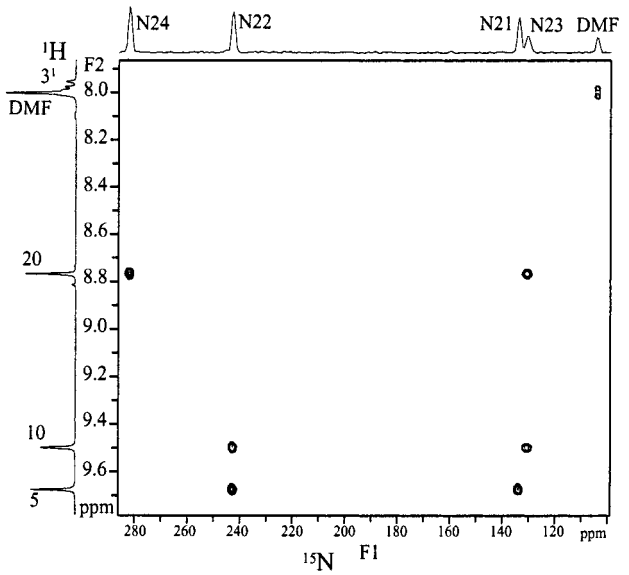

Figure 5. ^{1}H−^{15}N HMBC spectrum of chlorin **3**.

Table 2. ^{15}N Shifts of Chlorin Derivatives in $CDCl_3$ at 300 K

	^{15}N δ-values referenced to DMF (103.8 ppm)			
derivative	N_{21}	N_{23}	N_{22}	N_{24}
1[1]	131.5	128.5	-	281.5
2	129.3	134.3	242.5	287.9
3	130.2	133.5	243.0	282.0
4	130.9	134.9	250.4	281.1
5	132.3	132.7	250.0	284.3
6	126.5	134.5	242.1	298.0

way in the chlorin ring, and the electronic effects of the peripheral substituents. The ^{1}H−^{15}N heteronuclear NMR experiments were carried out at the natural abundance of ^{15}N by employing the HSQC and HMBC techniques. The ^{1}H−^{15}N HMBC spectrum of chlorin **3** in Figure 5 shows clear correlations between each nitrogen atom and its adjacent *meso*-protons. The ^{15}N signals for every chlorin (**2**−**6**) could be unambiguously assigned (Table 2) on the basis of correlations comparable with those shown for chlorin **3** in Figure 5. From Table 2, we can see that replacement of the C_7 methyl group in chlorin **3** with a formyl group (chlorin **4**) causes a noticeable 7.4 ppm deshielding effect in the δ_N of N_{22}. This deshielding can be attributed to the electron-withdrawing effect of the formyl group. The N_{24} of chlorin **6**, possessing the isocyclic ring *E*, gave the most deshielded δ_N value, whereas N_{21} produced the most shielded one, compared with the other chlorins. The prominent deshielding of N_{24} and shielding of N_{21} in chlorin **6** cannot be explained alone by the electron-withdrawing effects of the 13^1-oxo and the 13^2-methoxycarbonyl groups. We must also consider other relevant factors such as the conformational alterations induced in the macrocycle by the steric strain originating from the presence of the isocyclic ring.

Molecular Modeling. The heat of formation energies (ΔH_f and $\Delta\Delta H_f$) for the different NH tautomers (**A**−**F**) calculated by the PM3-UHF molecular modeling method are listed in Table 3 for chlorins **1**−**6**. The N_{21} and N_{23} protonated tautomer **A** exhibits the lowest energies for every derivative. The protonation of N_{24} interrupts the fully aromatic 18 π-electron delocalization pathway in the chlorin macrocycle and, therefore, raises the energy of tautomers **B**, **E**, and **F**. The addition of the isocyclic ring *E* influences strongly the tautomer energies, whereas the replacement of the 7-methyl group with a formyl group has an observable but a less pronounced effect (cf. the energies of **3** vs **4**).

The comparison of the bond angles and N−N distances (Tables 4 and 5) of the PM3-UHF optimized major tautomer (**A**) with the corresponding values of the X-ray structure,[11−13] shows good qualitative correlation for chlorins **2**, **3**, and **6**. Taking into account that the geometry-optimized monomer structures in a vacuum are not expected to be identical with the structures in packed crystals, the PM3-UHF modeling results are even quantitatively reasonable. The most rigid chlorin **6** shows the best equivalence between the structural parameters of the crystal and those of the PM3-UHF optimized molecule. In contrast, the more flexible chlorins **2** and **3** exhibit less equivalence between the parameters. It has been reported that the steric crowding in the lower periphery of crystalline **3** is released by distortions in the reduced subring *D*.[13,14] However, in the calculated model this ring is approximately coplanar with the macrocycle.

The energy-optimized **A**−**F** tautomers of chlorins **1**, **2**, **5** and **6** exhibit essentially planar chlorin-ring geometry. Nevertheless, in the corresponding tautomers of chlorins **3** and **4**, the subring *C* (likewise the C_{17} substituent) is tilted above the chlorin-ring plane defined by the four N atoms, the torsion angle (θ) of the C_{16}−C_{15}−C_{14}−C_{13} fragment being in the range 15−38°. The greatest torsion angle was observed for the **A** and **E** tautomers of chlorins **3** and **4**, θ being 31 and 38°, respectively. However, for the **B**−**D** and **F** tautomers of the same chlorins, θ was 22, 18, 17, and 15°, respectively, indicating higher chlorin-ring planarity. This is in agreement with the DNMR studies of chlorins **3** and **4**, showing that the rotation of the C_{15} substituent in the intermediate tautomer (**B** or **B′**) is hindered at lower temperatures. The smaller θ for the peripheral tautomers **B**−**D** (Scheme 1), indicates that ring *C* is more coplanar with the other subrings in these tautomers than in the major tautomer **A**. Consequently, the C_{13} substituent is pushed closer to the C_{15} substituent, which results in the hindered rotation of the 15-methoxycarbonylmethyl group.

We showed in our previous study of **1**[4] that the calculated spin-density maps lucidly illustrate the electron delocalization pathways in the chlorin ring. The spin-density maps in Figure 6 show the spin-polarization of the delocalized electrons in the chlorin **6** tautomers. It can be seen that the π-electrons of the vinyl group at C_3 delocalize actively with the π-electrons of the chlorin macrocycle. The electron delocalization of the C_{3^1}−C_{3^2} double bond is slightly more effective with an isolated C_2−C_3 double bond (**D**, Figure 6) than with the bond as a part of a fully aromatic 18-electron delocalization pathway (**A** and **C**). In all the modeled chlorins, the C_{3^1}−C_3 bond length is 1.43 Å, when the vinyl double bond neighbors an isolated C_2−C_3 double bond, and 1.44 Å, when the vinyl double bond conjugates directly to the aromatic pathway. In contrast, the 13^1-oxo group exhibits only a weak interaction with the aromatic C_{12}−C_{13} bond of tautomers **A** and **D** or with the isolated C_{12}−C_{13} double

(11) Senge, M. O.; Smith, K. M. *Z. Kristallogr.* **1992**, *199*, 239.
(12) Senge, M. O.; Ruhlandt-Senge, K.; Smith, K. M. *Acta Crystallogr., Sect. C* **1992**, *48*, 1810.
(13) Pajunen, A.; Stapelbroek-Möllmann, M.; Hynninen P. H. *Acta Crystallogr., Sect. C* **1996**, *52*, 743.
(14) Stapelbroek-Möllmann, M. Ph.D. Thesis, Universities of Helsinki and Bremen, 1997.

Table 3. PM3-UHF Optimized Heat of Formation (ΔH_f) Values of the Most Stable *trans*-Tautomers (A) and the Relative Energies of the Other Tautomers (B−F)

chlorin NH tautomer	ΔH_f of **A** and the $\Delta\Delta H_f$ [(**B**, **C**, **D**, **E**, or **F**) − (**A**)] of chlorins **1**−**6** in kcal/mol					
	1[4]	**2**	**3**	**4**	**5**	**6**
N_{21}−H, N_{23}−H (**A**)	−86.20	−67.21	−148.09	−171.73	−96.26	−13.35
N_{22}−H, N_{24}−H (**B**)	11.36	11.40	12.14	11.99	8.88	9.98
N_{21}−H, N_{22}−H (**C**)	7.03	6.64	8.44	8.13	7.71	4.70
N_{22}−H, N_{23}−H (**D**)	7.01	6.80	6.37	6.80	6.78	9.68
N_{23}−H, N_{4}−H (**E**)	17.71	17.89	17.23	17.47	16.10	16.95
N_{21}−H, N_{24}−H (**F**)	17.55	17.38	17.30	17.92	15.35	18.02

Table 4. Characteristic α Angle (C_{13}-C_{14}-C_{15}) for the PM3-UHF Optimized NH Tautomers of 1−6

chlorin NH tautomer	α (C_{13}−C_{14}−C_{15}) (deg)					
	1	**2**	**3**	**4**	**5**	**6**
N_{21}−H, N_{23}−H (**A**)	125.0	126.8 (129)[a,12]	128.9 (131)[a,13]	128.9	122.3	112.5 (114)[a,11]
N_{22}−H, N_{24}−H (**B**)	123.5	126.3	128.6	128.6	121.5	111.6
N_{21}−H, N_{22}−H (**C**)	124.1	125.0	127.3	127.3	120.9	111.1
N_{22}−H, N_{23}−H (**D**)	126.5	128.3	129.7	130.1	123.5	113.7
N_{23}−H, N_{24}−H (**E**)	124.9	126.8	128.8	128.7	122.2	112.5
N_{21}−H, N_{24}−H (**F**)	124.6	126.6	129.4	129.6	121.7	112.3

[a] Angles measured from X-ray structures.

bond of tautomers **B**, **C**, **E**, and **F** (Figure 6). In addition, the bond-length analysis shows that the C_{13}−C_{13^1} bond length is 1.47 Å in all the chlorin tautomers, indicating constant delocalization of the 13^1−C═O group with the chlorin π-electrons.

The substituent effects on the conformation of the chlorin macrocycle can be analyzed by assuming that the distant location of substituents in chlorin **2** ensures that its tautomers are free from substituent-induced ring strain. The conformationally illustrative C_{13}−C_{14}−C_{15} angle (α) varies between 125 and 128.3° in the tautomers of chlorin **2** and between 127.3 and 130.1° in the tautomers of chlorins **3** and **4** (Table 4). For all the modeled chlorins, the α angle is largest in the **D** tautomers and smallest in the **C** tautomers. The clearly smaller α value of 111.0−113.7° for the chlorin **6** tautomers implies that the presence of the isocyclic ring *E* induces ring strain into the chlorin macrocycle. The isocyclic ring *E* changes the minimum-energy conformations of the chlorin **6** macrocycle in the way that the **D** and **C** *cis*-tautomers become energetically clearly unequal (Table 3), as indicated by the 4.98 kcal/mol difference between the $\Delta\Delta H_f$ values for the **C** and **D** *cis*-tautomers of chlorin **6**. This is not the case for the **C** and **D** *cis*-tautomers of chlorins **1** and **2**, whose energies are similar, because the chlorins are free from steric crowding between the substituents in the lower periphery of the chlorin ring.

Inspection of the N−N interatomic distances in Table 5 shows that, in the chlorin **6** structures, the N_{21}−N_{22} and N_{23}−N_{24} distances are regularly longer and the N_{22}−N_{23} and N_{24}−N_{21} distances regularly shorter than the corresponding distances in the other chlorins. The low $\Delta\Delta H_f$ value of 4.70 kcal/mol for the **C** *cis*-tautomer of chlorin **6**, with a long N_{21}−N_{22} distance of 3.13 Å, implies weak steric repulsion between the two adjacent NH hydrogens (Table 5). In contrast, the clearly shorter N_{22}−N_{23} distance of 2.95 Å in the **D** *cis*-tautomer of the same chlorin can be interpreted to cause stronger steric repulsion between the adjacent NH hydrogens and hence to contribute to the higher $\Delta\Delta H_f$ value of 9.68 kcal/mol.

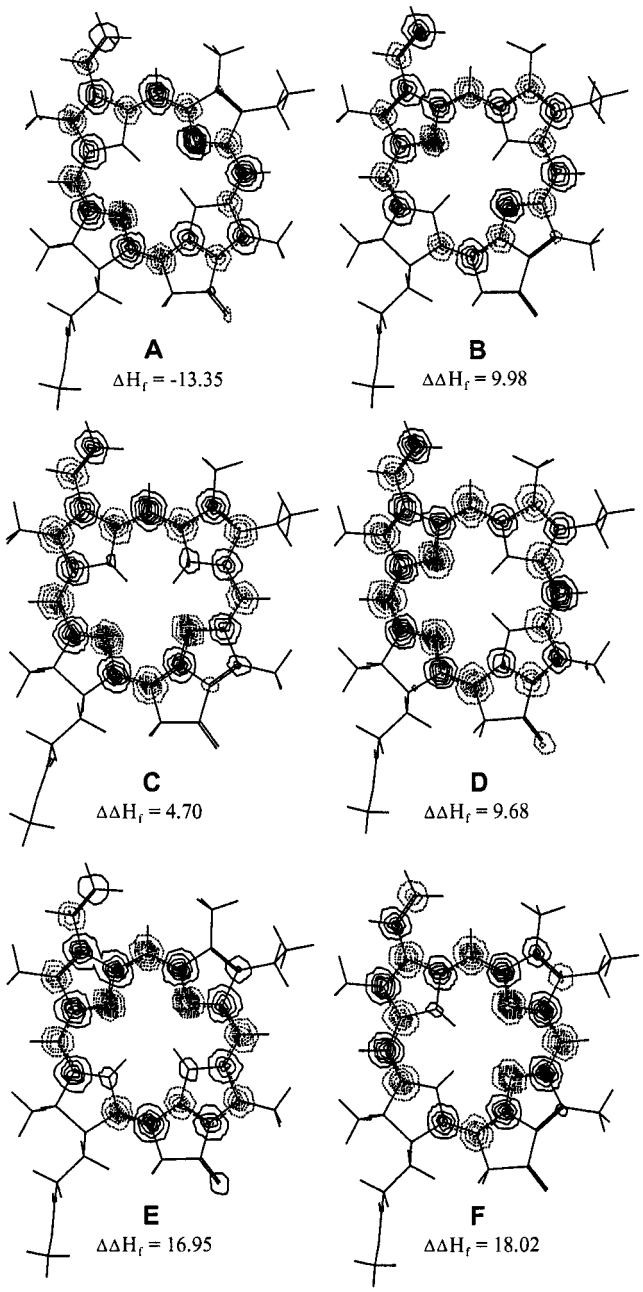

Figure 6. PM3-UHF optimized structures for the NH tautomers of **6** with spin-density contour maps. Broken and unbroken contour lines indicate opposite phases of polarized spins.

Discussion

The measured coalescence temperatures and calculated $\Delta G^{\ddagger}$ values varied notably depending on the chlorin substituents. The lowest $\Delta G_2^{\ddagger}$ were measured for the NH tautomeric exchange in chlorins **1** and **2**, which are essentially free from substituent-induced steric strain. The presence of the 15-methoxycarbonylmethyl substituent in chlorins **3** and **4** raised significantly the $\Delta G_2^{\ddagger}$ tautomerization barrier. In these chlorins, the steric

Table 5. PM3-UHF Optimized Distances between Nitrogen Atoms (Å) for the A−F Tautomers of Chlorins 1−6 (R_1 = $N_{21}-N_{22}$, R_2 = $N_{22}-N_{23}$, R_3 = $N_{23}-N_{24}$ and R_4 = $N_{21}-N_{24}$)[a]

chlorin NH tautomer	1				2				3				4				5				6			
	R1	R2	R3	R4	R1	R2	R3	R4	R1	R2	R3	R4	R1	R2	R3	R4	R1	R2	R3	R4	R1	R2	R3	R4
$N_{21}-H$, $N_{23}-H$					2.91[b]	2.93[b]	2.98[b]	2.95[b]	2.80	3.07	2.83	3.09									3.02	2.71	3.06	2.92
(X-ray)					2.90[c]	2.95[c]	2.96[c]	2.95[c]																
$N_{21}-H$, $N_{23}-H$ (**A**)	2.95	2.96	3.00	3.01	2.96	2.98	2.98	3.04	2.93	3.02	2.97	3.09	2.93	3.03	2.96	3.09	2.95	2.95	2.96	3.09	3.03	2.73	3.10	2.99
$N_{22}-H$, $N_{24}-H$ (**B**)	2.95	2.95	**3.01**	**2.99**	2.96	2.99	**2.96**	**3.03**	2.92	3.04	**2.93**	**3.06**	2.91	3.05	**2.91**	**3.08**	2.95	2.96	**2.94**	**3.08**	3.09	2.68	**3.11**	**2.95**
$N_{21}-H$, $N_{22}-H$ (**C**)	3.09	2.86	3.10	**2.91**	3.08	2.88	3.06	**2.96**	3.03	2.96	3.01	**3.01**	3.04	2.95	3.01	**3.00**	3.05	2.88	3.03	**3.01**	3.13	2.66	3.15	**2.94**
$N_{22}-H$, $N_{23}-H$ (**D**)	2.85	3.09	**2.91**	3.10	2.87	3.10	**2.90**	3.13	2.86	3.13	**2.90**	3.16	2.86	3.13	**2.90**	3.15	2.83	3.08	**2.87**	3.19	2.91	2.95	**2.99**	3.14
$N_{23}-H$, $N_{24}-H$ (**E**)	3.03	2.86	3.12	2.90	3.05	2.89	3.10	2.94	3.00	2.98	3.10	3.03	3.00	2.97	3.10	3.02	3.05	2.85	3.08	2.98	3.11	2.64	3.18	2.91
$N_{21}-H$, $N_{24}-H$ (**F**)	2.85	3.04	2.89	3.13	2.87	3.06	2.88	3.14	2.82	3.13	2.82	3.18	2.83	3.13	2.81	3.18	2.87	3.02	2.85	3.17	2.93	2.86	2.99	3.13

[a] For chlorins **2**, **3**, and **6** also the distances from X-ray structures are listed. Distances in the tautomers neighboring the hydrogen-bridged rate-limiting $\mathbf{TS_{BC}}$ and $\mathbf{TS_{BD}}$ (Scheme 2) are bold printed. [b] Triclinic crystal forms of **2**,[12] **3**,[13] and **4**.[11] [c] Orthorhombic crystal forms of **2**,[12] **3**,[13] and **4**.[11]

Scheme 2

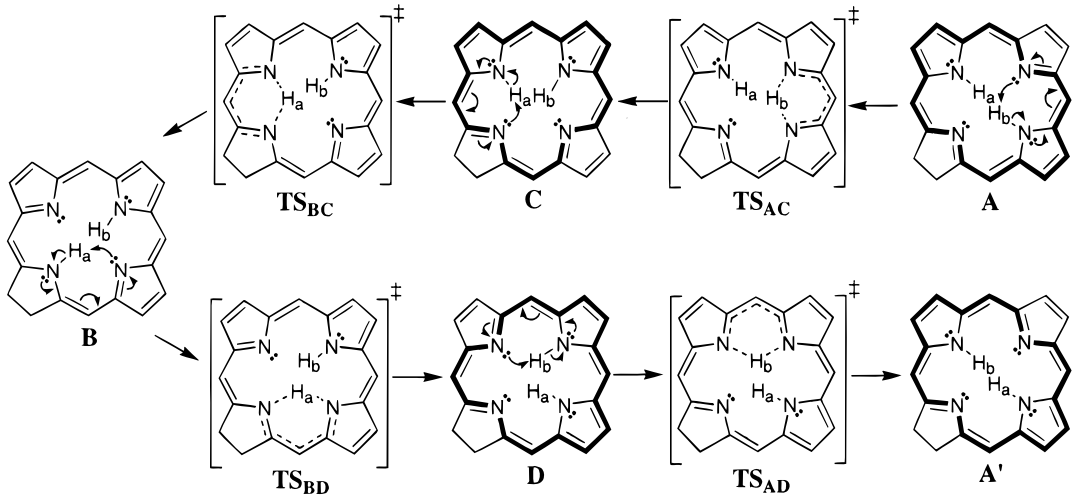

crowding among the bulky peripheral substituents at C_{13}, C_{15}, and C_{17} induces prominent steric strain, which is manifested in the optimized geometries of the chlorin tautomers, as was shown by the PM3-UHF calculations. The electronic effects of the formyl group in chlorin **4** lower the $\Delta G_1^{\ddagger}$ and $\Delta G_2^{\ddagger}$ values only by 0.2 and 0.3 kcal/mol, respectively, compared with the values of chlorin **3**.

The effects of the six-membered anhydride ring on the tautomeric process of chlorin **5** are similar to the effects induced by the C_{13} and C_{15} substituents in chlorins **3** and **4**. This is indicated by the very similar N−N distances and $\Delta G_2^{\ddagger}$ values for the three chlorins. In chlorin **6**, the presence of the isocyclic ring *E* induces anomalous bond lengths and angles in the chlorin macrocycle and, at the same time, rigidifies the macrocycle against skeletal deformations that are favorable for the tautomeric process.

At present, there is some general agreement that the total NH exchange in porphyrins occurs by a stepwise mechanism, but mechanistic considerations elucidating how a single transition state (TS) is formed in the pathway are rare in the literature. Relying on the measured H/D isotope effect, Abraham et al. have suggested a [1,5]-sigmatropic hydrogen-shift mechanism for the NH exchange in *meso*-tetraphenylporphyrin.[16] Sarai has suggested that "the proton tends to be attracted to the N···N line so as to form a hydrogen bond like structure".[17] We propose that the total NH exchange can proceed via two successive proton transfers, as depicted with arrows in Scheme 2. A neighboring nitrogen atom can initiate the transfer by donating an electron lone-pair to the proton moving in a hydrogen bridge. As a result, a hydrogen-bridged TS is formed in which 10 electrons reorganize in the six-membered cycle.

It is noteworthy that, in the proton-transfer mechanism depicted in Scheme 2, the $\mathbf{TS_{BD}}$ and $\mathbf{TS_{BC}}$ structures maintain aromaticity in the chlorin macrocycle. In this mechanism only the stepwise proton transfer is allowed, because the simultaneous formation of the two hydrogen-bridged $\mathbf{TS_{BD}}$ and $\mathbf{TS_{BC}}$ is not possible, assuming that delocalization in the chlorin macrocycle is largely preserved.

In trying to estimate the rate-limiting TS in the total NH tautomeric pathway for the investigated chlorins, we assume that the rate-limiting TS is located between the higher-energy *trans*-tautomer **B** and the adjacent fully aromatic *cis*-tautomer **C** or **D**. On the basis of Hammond's postulate, we may conclude that the rate-limiting TS ($\mathbf{TS_{BD}}$ or $\mathbf{TS_{BC}}$ in Scheme 2) resembles structurally more the *trans*-tautomer **B** than the *cis*-tautomers **C** or **D**. In addition, it seems reasonable to assume that a long hydrogen-bridged N−N distance in the TS structure is related to a high TS energy. We apply these principles to evaluate the rate-limiting TS energy barriers on the basis of the N−N distances (Table 5) in tautomers **B**−**D** for those nitrogens that form the hydrogen-bridge in $\mathbf{TS_{BC}}$ or $\mathbf{TS_{BD}}$. In the **B** *trans*-tautomer of chlorins **1** and **6**, the longest distance is between $N_{23}-N_{24}$ and assumes the values 3.01 and 3.11 Å, respectively, whereas in the **B** tautomer of chlorins **2**−**5** the longest distance is between $N_{21}-N_{24}$ and gets the values 3.03, 3.06, 3.08, and 3.08

(15) Hammond, G. S. *J. Am. Chem. Soc.* **1955**, *77*, 334.
(16) Abraham, R. J.; Hawkes, G. E.; Smith, K. M. *Tetrahedron Lett.* **1974**, *16*, 1483.
(17) Sarai, A. *Chem. Phys. Lett.* **1981**, *83*, 50.

Å, respectively. This leads us to the conclusion that the rate-limiting barrier for the total NH exchange should be the highest for chlorin **6** (**TS$_{BD}$**, Scheme 2) and lowest for chlorins **1** (**TS$_{BD}$**) and **2** (**TS$_{BC}$**), whereas for chlorins **3**−**5** (**TS$_{BC}$**), the barrier should lie between the two extremes. This is in a good agreement with the experimentally measured activation free energies (Table 1).

The higher-energy *trans*-tautomer **B** observed for chlorins **3** and **4** is lying between the two transition states, **TS$_{BC}$** and **TS$_{BD}$** (Scheme 2), but only the formation of **TS$_{BC}$** is shown by the static N−N distance analysis. Apparently, the second barrier ($\Delta G_1^{\ddagger}$) of chlorins **3** and **4** originates from such a structural factor, which increases steric strain in the lower part of the macrocycle and raises the **TS$_{BD}$** energy. Only the major tautomer **A** and one energy barrier ($\Delta G_2^{\ddagger}$) was observed for chlorin **5**, despite that the probabilities of the formation of **TS$_{BC}$** and **TS$_{BD}$** should be about equal for chlorins **3**−**5** as judged from the N−N distance parameters. It seems reasonable to assume that the anhydride ring of chlorin **5** allows such in-plane macrocyclic deformations, which enable N_{23} and N_{24} to approach each other but that in chlorins **3** and **4** these types of deformations are not allowed because of strongly increased steric crowding between the C_{13} and C_{15} substituents.

In the case of symmetrically substituted porphyrins a strong connectivity has been found between NH tautomerism and skeletal vibrations.[17,18] The NH exchange can be expected to occur preferably via the macrocycle conformations enabling short N−N distances. In chlorins **3**−**6**, the restraints in the lower periphery of the macrocycle can, in principle, hinder the N_{23} and N_{24} atoms from approaching each other in the dynamic chlorin skeleton deformations. The restraints should be the highest for chlorin **6**, in which the chemical strain, induced by the isocyclic ring *E*, freezes the macrocycle conformation effectively. Despite that the N_{22}−N_{23} distance in the **A** and **C** tautomers is short, 2.73 and 2.66 Å, respectively, and that the $\Delta\Delta H_f$ value of the **C** *cis*-tautomer is only 4.70 kcal/mol (Tables 3 and 5), there is no experimental evidence for the NH exchange between these tautomers in chlorin **6**. This supports the theory that the skeletal motions in the chlorin macrocycle are connected to the NH tautomerism and that the hindrance of these motions raises the tautomerization barriers.

Complete assignments for ^{1}H NMR spectra of the intermediate tautomers observed for **3** and **4** could not be achieved, because we could not apply the heteronuclear NMR techniques at lower temperatures. Nevertheless, the high-field shifts of the 5 and 20 *meso*-proton signals as well as the low-field shifts of the NH proton signals, assigned with certainty for chlorin **4** (Figure 3), indicate that the ring-current is weakened in the observed intermediate, which is consistent with the reduced aromaticity of the *trans*-tautomer **B**. The prominent changes in the form of the 15^1-CH_2 proton signal can be interpreted as a sign of increased nonequivalency of these methylene protons in the observed intermediate tautomer. The 15^1-CH_2 protons became nonequivalent because the rotations of the C_{15} methoxycarbonylmethyl group were slowed in the tautomer **B** by the adjacent C_{13} methoxycarbonyl substituent. The increased deshieldings of the 15^1-CH_2 protons (Figure 3) could originate from the deshielding cone of the C_{13^1} carbonyl group.

In conclusion, the NMR and molecular modeling results proved that the chlorin-ring substituent effects are connected to the NH tautomeric exchange. The lowest $\Delta G_2^{\ddagger}$ values were measured for the exchange in chlorins **1** and **2**, which are essentially free from substituent-induced steric strain. Raised $\Delta G_2^{\ddagger}$ values were obtained for chlorins **3** and **4**, in which substituent-induced steric strain was indicated by molecular modeling. The higher-energy *trans*-tautomer **B** of **3** and **4**, trapped at lower temperatures, proved that intermediate NH tautomers of chlorins can be present in observable amounts in solution. The effect of the six-membered anhydride ring in chlorin **5** on the $\Delta G_2^{\ddagger}$ barrier was comparable to the effect of the C_{13} and C_{15} substituents in chlorins **3** and **4**. The five-ring *E* in chlorin **6** distorted and rigidified the macrocycle, and therefore, no NH exchange was experimentally observed. A stepwise tautomerization mechanism (Scheme 1) is suggested to proceed so that a neighboring nitrogen atom initiates the NH transfer by donating an electron lone-pair to the proton moving in a hydrogen bridge. This implies the formation of a hydrogen-bridged TS, in which 10 electrons reorganize in a six-membered cycle (Scheme 2).

Experimental Section

Preparation of Chlorins 2−6. The syntheses of chlorins **2**−**5** have been described in detail elsewhere.[13,14] 3^1,3^2-Didehydrophytochlorin methyl ester (**6**) was prepared from 13^2-demethoxycarbonylchlorophyll *a*[19] by transesterification and demetalation, using 5% H_2SO_4 in methanol.[20]

NMR Spectra. All the NMR spectra were recorded on a Varian Unity 500 spectrometer, with the exception that the DNMR spectra of chlorin **6** in pyridine-d_5 were measured on a Varian INOVA 300 instrument. The variable-temperature (DNMR) ^{1}H spectra were measured from 6−12 mg of compound **2**−**6** in a 5 mm NMR tube using a 0.6 mL sample volume; the spectra were referenced to internal TMS (0.00 ppm). $CDCl_3$ (Euriso-top, 99.96% D), DMSO-d_6 (Merck, 99% D), CD_3CN (Aldrich, 99% D), and pyridine-d_5 (Euriso-top, 99.5% D) were taken from ampules, and 1,4-dioxane-d_8 (Fluka, 99.5% D) was from a sealed bottle. The ^{1}H signals of methanol and ethylene glycol (100%, Varian test samples) were used for low- and high-temperature calibrations, respectively. The variable-temperature ^{1}H spectra were recorded using an acquisition time of 4 s with a 1 s delay between the 64−128 recorded scans.

The conditions of the heteronuclear ^{1}H−^{15}N HSQC and HMBC experiments are described in detail in our previous paper.[4] The sample concentrations in the heteronuclear measurements were 0.05−0.06 M in $CDCl_3$ (purity as above). A 5 mm Shigemi tube was used to adjust the sample volume down to 0.2 mL. A small amount (ca. 1 μL) of DMF (Merck, 99.5%, dried with 4 Å molecular sieves, BDH) was used as internal standard (δ_N 103.8) for the ^{15}N chemical shifts in the HMBC experiment.

Molecular Modeling. The PM3-UHF molecular geometry optimizations[21] were performed on a Pentium II 300 MHz PC computer using the HyperChem (4.5) software package.[22] The full optimization of geometry was achieved for the NH tautomers of **2**−**6** using 206, 230, 232, 206, and 200 molecular orbitals, respectively, in the semiempirical calculations. The structures were energy-optimized by employing the Polak-Ribiere conjugate gradient optimization algorithm with an energy convergence criterion of 0.01 kcal Å^{-1} mol^{-1}.

JO9918955

(18) Sarai, A. *J. Chem. Phys.* **1984**, *80*, 5341.
(19) Hynninen, P. H.; Lötjönen, S. *Synthesis* **1980**, 539.
(20) Tauber, A. Y.; Kostiainen, R. K.; Hynninen, P. H. *Tetrahedron* **1994**, *50*, 4723.
(21) Stewart, J. J. P. *J. Comput. Chem.* **1989**, *10*, 208.
(22) HYPERCHEM, Hypercube, http://www.hyper.com.